Published in final edited form as:
Dev Dyn. 2011 October ; 240(10): 2309–2323. doi:10.1002/dvdy.22735.

The tight junction scaffolding protein cingulin regulates neural crest cell migration

Chyong-Yi Wu[§], **Sharon Jhingory**[§], and **Lisa A. Taneyhill**[*]
Department of Animal and Avian Sciences, University of Maryland, College Park, MD 20742, USA

Abstract

Neural crest cells give rise to a diverse range of structures during vertebrate development. These cells initially exist in the dorsal neuroepithelium and subsequently acquire the capacity to migrate. Although studies have documented the importance of adherens junctions in regulating neural crest cell migration, little attention has been paid to tight junctions during this process. We now identify the tight junction protein cingulin as a key regulator of neural crest migration. Cingulin knock-down increases the migratory neural crest cell domain, which is correlated with a disruption of the neural tube basal lamina. Overexpression of cingulin also augments neural crest cell migration and is associated with similar basal lamina changes and an expansion of the premigratory neural crest population. Cingulin overexpression causes aberrant ventrolateral neuroepithelial cell delamination, which is linked to laminin loss and a decrease in RhoA. Together, our results highlight a novel function for cingulin in the neural crest.

Keywords

cingulin; tight junctions; neural crest; EMT; delamination; migration; RhoA

INTRODUCTION

The neural crest is a transient population of migratory cells that differentiates to form a variety of cell types in the vertebrate embryo, including melanocytes, the craniofacial skeleton, and components of the peripheral nervous system (Kalcheim and Le Douarin, 1999). Initially residing in the dorsal neural tube as adherent cells (and termed the premigratory neural crest), these cells undergo an epithelial-to-mesenchymal transition (EMT), characterized by the loss of intercellular contacts and the generation of motile, mesenchymal neural crest cells (Hay, 1995). The acquisition of motility by premigratory neural crest cells is requisite for these cells to develop into appropriate structures and contribute to the formation of a fully functional vertebrate embryo.

The EMTs that underlie both normal (gastrulation, neural crest emigration) and aberrant (metastasis) processes (Leptin et al., 1992; Thiery, 2002; Hemavathy et al., 2004) are quite similar at the molecular level, and involve the dismantling of both cellular adherens and tight junctions in order to promote cell movement (Hemavathy et al., 2000; Nieto, 2002; Ikenouchi et al., 2003; Ohkubo and Ozawa, 2004; Barrallo-Gimeno and Nieto, 2005; De Craene et al., 2005; Perez-Mancera et al., 2005; Martinez-Estrada et al., 2006; Taneyhill et al., 2007; Wu and McClay, 2007; Sauka-Spengler and Bronner-Fraser, 2008; Yang and

[*]Corresponding author. Address for manuscript correspondence: Lisa A. Taneyhill, Ph.D., 1405 Animal Sciences Center, University of Maryland, College Park, MD 20742, USA, Tel: 301 405 0597, Fax: 301 405 7980, ltaney@umd.edu.
[§]These authors contributed equally to this work.

Weinberg, 2008; Acloque et al., 2009; Ahlstrom and Erickson, 2009). Prior studies have shown that the repression of *cadherins*, such as epithelial *cadherin* (*E-cadherin*) and *cadherin6B* (*Cad6B*), and tight junction components, including *claudins* and *occludins*, is critical to facilitate EMTs. Known as zonula occludens, tight junctions exist at the most apical region of cells, almost completely lack intercellular membrane space, and function as a semi-permeable size- and ion-specific barrier, thereby constraining the movement of molecules between the apical and basolateral surfaces of the cell (Niessen, 2007). Transmembrane components of tight junctions consist of the junctional adhesion molecules claudins and occludins, while cytoplasmic proteins, such as zonula occludens and cingulin, play important roles in mediating the interactions among the transmembrane components of the tight junction and provide connections to the cytoskeleton (Niessen, 2007).

Down-regulation of some tight junction components has been reported to occur during neural tube closure and in premigratory neural crest cells during the initiation of EMT (Aaku-Saraste et al., 1996; Sauka-Spengler and Bronner-Fraser, 2008). As a first step in investigating the function of specific tight junction proteins in neural crest cell ontogeny, we have characterized the role of cingulin, a tight junction scaffolding protein. Cingulin is expressed in the developing midbrain neural crest cell population but is absent in migratory neural crest cells. Depletion and overexpression of cingulin increases the migratory neural crest cell population and is associated with additional loss of laminin surrounding the neural tube. The increase in migratory neural crest cells observed upon cingulin overexpression occurs through the expansion of the premigratory neural crest domain. In the ventrolateral neuroepithelium, cingulin overexpression causes ectopic delamination of cells and can be correlated with a loss of the Rho GTPase RhoA. Effects of cingulin in premigratory neural crest cells in the dorsal neural tube, however, appear to be independent of any changes in RhoA. Collectively, our studies indicate that cingulin is important for midbrain neural crest cell migration in the developing chick embryo.

RESULTS

Cingulin is apically distributed in the neural tube but is absent from migratory neural crest cells

We determined the spatio-temporal distribution of cingulin protein during neural crest cell development in the chick embryo midbrain. Whole-mount immunohistochemistry for cingulin protein followed by transverse sectioning reveals that cingulin is localized to the apical region of the neural tube as early as the 4 somite stage (ss) (Fig. 1A, C, D, F, G, I, J, L, M, P asterisks), an expected site given its association with tight junctions (Niessen, 2007). At the 8ss, however, HNK-1-positive migratory neural crest cells are devoid of cingulin protein (Fig. 1O, P, arrowheads). In addition, cingulin is found more diffusely throughout the dorsal neural tube at both the 7ss and 8ss (Fig. 1J, L, M, P, arrows). Taken together, these results indicate that cingulin protein is localized in the proper spatio-temporal pattern to play a potential role in neural crest cell development in the chick midbrain.

Depletion of cingulin expands the size of the migratory neural crest cell domain and is correlated with dorsal loss of basal lamina

To delineate a functional role for cingulin in the neural crest, we designed a morpholino antisense oligonucleotide (MO) to target and knock-down *cingulin* mRNA translation, thus depleting cingulin protein levels in the chick premigratory neural crest cell population. Using the method of *in ovo* electroporation (Itasaki et al., 1999; Jhingory et al., 2010), we transfected chick midbrain neural tube cells with either *Cingulin* MO or a 5 base pair mismatch *Cingulin* control MO (hereafter referred to as control MO). This control MO has no effect on cingulin protein levels in the neural tube (Fig. 2A, D, arrows; 12/12 embryos).

Electroporation of *Cingulin* MO depletes cingulin protein in the neural tube after an 8 hour incubation with the MO (Fig. 2E, H, arrows; 11/12 embryos).

To assess any differences in the migratory neural crest cell population, embryos were electroporated with either *Cingulin* or control MO, re-incubated for 8 hours, and then processed for whole-mount *in situ* hybridization for *Sox10*, *Snail2*, and *FoxD3*, or immunostained using an antibody to HNK-1. Treatment with control MO has no effect on *Sox10* (Supp. Fig. 1A, B; 8/8 embryos), *Snail2* (Supp. Fig. 1C, D; 10/11 embryos), *FoxD3* (Supp. Fig. 1E; 13/13 embryos), and HNK-1 immunostaining (Supp. Fig. 1F; 9/9 embryos). Depletion of cingulin from the premigratory neural crest, however, leads to an increase in the size of the *Sox10*-positive migratory neural crest cell domain on the transfected side (right) of the embryo, compared to the contralateral control side (and to control embryos) (Fig. 2I, J, arrow; 13/14 embryos). We confirmed this increase by counting the number of *Sox10*-positive migratory neural crest cells on both the treated and contralateral control sides in sectioned embryos. We find a 1.4-fold increase in the number of *Sox10*-positive migratory neural crest cells upon depletion of cingulin (*Cingulin* MO: 210 +/− 19, contralateral control side: 147 +/−11; Student's *t* test of $p < 0.000001$; see Fig. 2T). No change in the number of *Sox10*-positive migratory neural crest cells was observed upon treatment with the control MO (control MO: 180 +/−8; contralateral control side: 180 +/−8). We also examined expression of *Snail2* and *FoxD3*, both molecular markers of premigratory and migratory cranial neural crest cells, and we observe a similar increase in the size of the *Snail2*- (Fig. 2K, L, arrow; 12/14 embryos) and *FoxD3*-(Fig. 2M, arrow; 9/12 embryos) positive migratory neural crest cell domain on the transfected side compared to the contralateral control side. This phenotype is also evident in embryos that have undergone immunostaining for the migratory neural crest cell marker HNK-1 (Fig. 2N, arrow; 8/11 embryos).

We next assessed effects of cingulin knock-down on neural crest cell migration at both early (3 hours) and later (20 hours) time points post-electroporation. Depletion of cingulin at both of these time points reduces the amount of cingulin protein observed in the neural tube (data not shown). MO-mediated knock-down of cingulin for 3 hours results in an increase in the *Sox10*-positive migratory neural crest cell domain at stages of embryonic development during which neural crest cell emigration is just initiating (Fig. 2O, P, arrow; 10/11 embryos). Furthermore, long-term depletion of cingulin leads to the presence of more *Sox10*-positive migratory neural crest cells in the head region of the embryo, an observation not noted on the contralateral control side or in control embryos (Fig. 2Q, R, arrow; 10/11 embryos).

In order to ensure that the increase in the migratory neural crest cell domain observed upon cingulin knock-down was not due to changes in cell proliferation in the neural tube or in the migratory neural crest cell population, we performed phospho-histone H3 (PH3) immunostaining on transverse sections taken from embryos treated with *Cingulin* or control MO for 8 hours. No considerable difference in cell proliferation is observed in the presence of either MO, compared to each other and to the contralateral control side of the embryo (Supp. Fig. 2A, B, arrowheads). In addition, no change in the amount of cell death is noted by TUNEL assay 8 hours after treatment with either MO (Supp. Fig. 2C, D, arrowheads). The increased number of migratory neural crest cells observed at both 3 and 20 hours upon *Cingulin* MO treatment is also not due to any considerable differences in cell proliferation or cell death (data not shown).

To determine if the increase in the migratory neural crest cell domain was due to changes in the premigratory neural crest cell population, we examined younger embryos at premigratory stages prior to neural fold fusion. We observe no appreciable difference in the expression of the premigratory neural crest cell markers *FoxD3* (Fig. 2S, arrow; 7/7

embryos) and *Snail2* (6/6 embryos; data not shown) in the neural folds of embryos treated with *Cingulin* or control MO. To confirm this observation, we counted the number of *FoxD3*- and *Snail2*-positive premigratory neural crest cells on both MO-treated and contralateral control sides of sectioned embryos. We find no change in the number of premigratory neural crest cells upon knock-down of cingulin (*FoxD3: Cingulin* MO: 56 +/−6, contralateral control side: 60 +/−6; *Snail2: Cingulin* MO: 67 +/−5, contralateral control side: 68 +/−5; see Fig. 2T) or upon introduction of the control MO (data not shown).

Given the enhanced emigration and/or migration phenotype we observe upon cingulin knock-down, we checked cingulin-depleted embryos for potential effects on the basal lamina and cellular junctions. Cingulin knock-down results in additional dorsolateral loss of basal lamina at stages of development when active neural crest cell emigration is about to commence, as assessed by immunostaining for the protein laminin (Fig. 3A, D; arrows, 6ss; 13/15 embryos). Furthermore, we observe persistent loss of laminin more dorsolaterally on the electroporated side of older embryos at axial levels in which the basal lamina has become continuous on the contralateral control side, after cessation of neural crest cell emigration (Fig. 3E, H, arrows, 10ss; 9/10 embryos). We note no change, however, in the premigratory neural crest-specific Cadherin, Cad6B (Fig. 3I, L, arrows; 7/7 embryos), or in the levels of claudin-1, a transmembrane tight junction component (Fig. 3M, P, arrows; 8/10 embryos), or ZO-1, another tight junction scaffolding protein (9/9 embryos; data not shown), on the side of the neural tube in which cingulin has been depleted. Finally, examination of the dorsal neural tube at higher resolution reveals that neural crest cells emigrate from more dorsolateral positions of the neural tube upon cingulin knock-down (Fig. 3R, T, arrowheads), an observation that is associated with reduction of laminin in this region (Fig. 3Q, T, arrows). Collectively, our results indicate that depletion of cingulin expands the migratory neural crest cell population, a phenotype correlated with disruption of the basal lamina and emigration of cells from more dorsolateral positions in the neural tube, but through a mechanism independent of gross changes in cellular junctions.

Forced expression of cingulin increases the size of the migratory neural crest cell population through changes in the premigratory neural crest domain and causes ectopic delamination within the neuroepithelium

We next overexpressed cingulin in the developing neuroepithelium of the chick midbrain and monitored for any changes in neural crest cell migration. We cloned the full-length *cingulin* cDNA into the pCIG expression vector (pCIG-Cingulin) and then introduced the construct (or the control pCIG vector) into the chick midbrain by electroporation. The control pCIG construct has no effect on cingulin protein distribution (Fig. 4A, D, arrows; 11/11 embryos), whereas overexpression of cingulin results in up-regulation of cingulin protein 1) throughout the apical region of the transfected side of the neural tube (Fig. 4E, H; 9/9 embryos), 2) in the nucleus (Fig. 4E, H, carets), and 3) along the lateral edges of neuroepithelial cells (Fig. 4E, H, arrows). These latter two phenotypes constitute aberrant distribution patterns for cingulin protein (see Fig. 1). In addition, cingulin overexpression leads to the inappropriate distribution of cells 1) in the neural tube lumen (Fig. 4E, H, arrowheads) and 2) outside of the neural tube at more ventral, and thus ectopic, locations (Fig. 4E, H, asterisks).

To assess potential effects on neural crest cell development, we electroporated the control pCIG or pCIG-Cingulin construct independently into the developing neural crest cell population of the chick midbrain, re-incubated the embryos for 8 hours, and then processed them for whole-mount *in situ* hybridization for *Sox10*, *Snail2*, and *FoxD3*, or for immunostaining using an antibody to HNK-1. Treatment with pCIG has no effect on *Sox10* (Supp. Fig. 3A, B; 10/10 embryos), *Snail2* (Supp. Fig. 3C, D; 10/10 embryos), *FoxD3* (Supp. Fig. 3E; 8/10 embryos), and HNK-1 immunostaining (Supp. Fig. 3F; 8/8 embryos).

Overexpression of cingulin, however, perturbs neural crest cell development, as evidenced by the distribution of *Sox10*- (Fig. 4I, J, arrow; 9/10 embryos), *Snail2*- (Fig. 4K, L, arrow; 11/12 embryos), *FoxD3*- (Fig. 4M, arrow; 9/10 embryos), and HNK1-positive (Fig. 4N, arrow and arrowhead; 10/11 embryos) migratory neural crest cells observed on the transfected side of the embryo, compared to the contralateral control side (and to control embryos). Neural crest cells emigrate properly from the neural tube, but we often see cells present in the neural tube lumen that are either negative (Fig. 4J, L, M, arrowheads) or positive (Fig. 4N, O, P, arrowheads) for neural crest cell molecular markers. We also detect an expansion of the migratory neural crest cell population on the transfected side of the embryo compared to the contralateral control side, a phenotype similar to our cingulin-depleted embryos (Fig. 4I–P, arrows). To corroborate this expansion, we counted the number of *Sox10*-positive migratory neural crest cells on both the treated and contralateral control sides of sectioned embryos. We find a 1.8-fold increase in the number of *Sox10*-positive migratory neural crest cells upon overexpression of cingulin (pCIG-Cingulin: 179 +/−12, contralateral control side: 108 +/−7; Student's *t* test of $p < 0.0000001$; see Fig. 4R). No change in the number of *Sox10*-positive migratory neural crest cells was observed upon treatment with the pCIG control vector (pCIG: 192 +/−11; contralateral control side: 185 +/−12). Finally, we often detect changes in neural tube architecture on the electroporated side following neural fold fusion upon overexpression of cingulin (Fig. 4J, L, M, N, P; asterisks).

We next assessed effects of cingulin overexpression on neural crest cell migration at a later time point post-electroporation. Overexpression of pCIG-Cingulin and fixation of embryos after 20 hours of incubation causes similar phenotypic changes in cingulin protein distribution to those observed after 8 hours (data not shown). Examination of embryos overexpressing cingulin reveals the presence of *Sox10*-positive migratory neural crest cells within the neural tube lumen (Fig. 4O, P, arrowheads; 13/14 embryos). We also observe additional migratory neural crest cells in a more dorsal position on the transfected side of the embryo (Fig. 4P, arrow) compared to the contralateral control side (and to control embryos, data not shown).

In order to ensure that the change in the number of migratory neural crest cells observed upon cingulin overexpression was not due to differences in cell proliferation in the neural tube or in the migratory neural crest cell population, we performed PH3 immunostaining on embryos electroporated with pCIG or pCIG-Cingulin and incubated for 8 hours. No appreciable difference in cell proliferation is observed in the presence of either construct, compared to each other and the contralateral control side of the embryo (Supp. Fig. 4A, B, arrowheads). In addition, no change in the amount of cell death in the neuroepithelium is noted by TUNEL assay upon treatment with either construct (Supp. Fig. 4C, D, arrowheads), although some cells that inappropriately enter the neural tube lumen eventually undergo apoptosis and become TUNEL-positive (Supp. Fig. 4D, arrows). The increase in the migratory neural crest cell population observed after 20 hours of cingulin overexpression is also not due to any changes in cell proliferation or cell death (data not shown).

The increase in and effects on migratory neural crest cells that we observe upon cingulin overexpression at both early and later time points in development led us to examine whether any differences in the premigratory neural crest domain in the dorsal neural tube could be noted. In young embryos prior to neural fold fusion, we detect the expansion of the premigratory neural crest cell population on the transfected side of the neural tube compared to the contralateral control side, ascertained by examining two markers of premigratory neural crest cells, *FoxD3* (Fig.4Q, arrow; 9/11 embryos) and *Snail2* (7/8 embryos; data not shown). To corroborate this change, we counted the number of *FoxD3*- and *Snail2*-positive premigratory neural crest cells on both the treated and contralateral control sides in sectioned embryos. We find a statistically significant increase in the number of premigratory

neural crest cells in the dorsal neural tube upon overexpression of cingulin (*FoxD3*: pCIG-Cingulin: 65 +/−5, contralateral control side 42 +/−3; 1.6-fold increase, Student's *t* test of $p < 0.00001$; *Snail2*: pCIG-Cingulin: 42 +/−4, contralateral control side: 31 +/−3, 1.4-fold increase, Student's *t* test of $p < 0.0001$; see Fig. 4R). No change in the number of premigratory neural crest cells was noted upon electroporation of the pCIG control vector (data not shown).

The presence of cingulin-positive cells outside of the neural tube epithelium at more ventral locations (see Fig. 4E, H, asterisks) led us to next investigate the distribution of laminin. Overexpression of cingulin leads to ectopic loss of laminin throughout multiple regions within the transfected side of the neural tube (Fig. 5A, D, arrows; 8/9 embryos), including the dorsal region (Fig. 5A, D, asterisks). Moreover, we observe no change in the distribution of Cad6B protein in the premigratory neural crest domain of the dorsal neural tube (Fig. 5E, H, arrows; 8/9 embryos) or in the localization of claudin-1 (Fig. 5I, L, arrows; 10/10 embryos) or ZO-1 (11/11 embryos; data not shown). Finally, examination of the dorsal neural tube at higher magnification reveals that neural crest cells emigrate from more dorsolateral positions of the neural tube (Fig. 5N, P, arrowheads) after cingulin overexpression, which is consistent with the expanded premigratory neural crest domain and further loss of laminin (Fig. 5M, P, arrows). Taken together, these data suggest that the regulation of neuropithelial cell delamination by cingulin is associated with changes in laminin, and, in the case of neural crest cells, involves the expansion of the premigratory neural crest cell domain.

Cingulin modulates RhoA levels in the ventrolateral, but not dorsal, neuroepithelium, with loss of RhoA correlating with ectopic ventrolateral cell delamination

Given that cingulin has been shown to negatively regulate the Rho GTPase RhoA (Guillemot and Citi, 2006; Citi et al., 2009), and the general importance of Rho proteins in mediating various types of developmental EMTs (Liu and Jessell, 1998; Groysman et al., 2008; Nakaya et al., 2008), we next explored potential effects on RhoA distribution after perturbation of cingulin. We performed immunohistochemical staining for RhoA on transverse sections taken through the chick midbrain region after 8 hours of *Cingulin* MO incubation. We observe a 1.8-fold increase in RhoA protein along the apical surface of the ventrolateral region of the neural tube in cingulin-depleted embryos, compared to the contralateral control side of the embryo (Fig. 6A, D, arrows; Student's *t* test of $p < 0.0000001$). All embryos show a decrease in apical RhoA protein in the dorsal neural tube, however, during stages of active neural crest cell emigration and migration (Fig. 6A, D, asterisks), as described previously (Kinoshita et al., 2008). Conversely, RhoA protein is absent (no signal detected above background) from the apical region of the ventrolateral neural tube upon overexpression of cingulin (Fig. 6E, H, arrows). Again, RhoA levels in the premigratory neural crest region of the dorsal neural tube are impervious to changes in cingulin and are decreased (Fig. 6E, H, asterisks). Finally, the loss of RhoA in the ventrolateral region of the neuroepithelium correlates with the ectopic delamination that we observe after cingulin overexpression (Fig. 5A, D, arrows). Collectively, these results indicate that a decrease in RhoA is associated with aberrant basal lamina breakdown in the ventrolateral neuroepithelium upon forced expression of cingulin, but that RhoA levels in the dorsal neural folds/tube are not altered by perturbation of cingulin.

DISCUSSION

Cingulin protein is distributed apically in the developing chick midbrain neuroepithelium and is absent in migratory neural crest cells

Known as zonula occludens, tight junctions exist at the most apical region of epithelial cells and function as a “fence” to constrain the movement of molecules between the apical and basolateral membranes (Niessen, 2007). Cingulin, a peripheral tight junction component, was originally discovered in brush border cells of the chick intestine (Citi et al., 1988) and is observed in other polarized epithelial and endothelial tissues but is notably absent from mesenchymal and myogenic cell types (Citi et al., 1989). Cingulin interacts with other tight junction components, as well as myosin and actin, thus providing a potential link to the cytoskeleton (Cordenonsi et al., 1999; D’Atri and Citi, 2001; D’Atri et al., 2002). Cingulin-rich tight junctions have been identified via immunohistochemistry during the early stages of mouse development (Fleming et al., 1993; Javed et al., 1993) and *Xenopus laevis* embryogenesis (Cardellini et al., 1996; Fesenko et al., 2000; Cardellini et al., 2007). In late morula and early blastocyst mouse embryos, prospective trophectoderm cells also possess peri-nuclear cingulin cytoplasmic foci, consistent with cingulin localization to endocytic vesicles that are believed to promote cingulin degradation (Fleming et al., 1993).

In the developing chick midbrain, we find cingulin protein localized to the midbrain ectoderm and endoderm as early as the 4ss of chick development, as well as specific expression in the apical region of the neural tube. Neural crest cell progenitors, or premigratory neural crest cells, reside in the dorsal aspect of the pseudo-stratified neural tube epithelium, and, as such, are cingulin-positive throughout their development in the chick midbrain. At initial stages of EMT (7ss), cingulin protein is maintained in more apical-ventral regions of the neuroepithelium, while the apical membrane distribution of cingulin in neural crest cell progenitors in the dorsal neural tube is somewhat diminished, even though cingulin protein itself is still present dorsally. This expression pattern persists during active neural crest cell migration at the 8ss during which time neural crest cell progenitors are emigrating from the neural tube. Newly delaminated, migratory (i.e. HNK-1-positive) neural crest cells, however, lack cingulin protein, consistent with a previously published report indicating that cingulin is absent from mesenchymal cell types (Citi et al., 1989) as well as the finding that migratory neural crest cells down-regulate components of tight junctions (Sauka-Spengler and Bronner-Fraser, 2008). Therefore, cingulin is expressed in the proper spatio-temporal pattern to potentially play a role in regulating neural crest cell development.

Depletion of cingulin expands the migratory neural crest cell population *in vivo* and is associated with changes in the basal lamina

To investigate a possible function for cingulin in the developing midbrain neural crest cell population, we depleted cingulin using MO-mediated knock-down. Cingulin knock-down leads to an increase in the size of the migratory neural crest cell domain at multiple time points post-electroporation of the *Cingulin* MO, as assessed by the expression of a variety of different neural crest cell molecular markers. This phenotype is not due to any changes in cell proliferation or cell death (in the neural tube or migratory neural crest cell population), or in the number of premigratory neural crest cells observed in the dorsal neural tube. Interestingly, we observe additional loss of laminin, a component of the basal lamina surrounding the neural tube, in the dorsolateral region neural tube. In older embryos where the basal lamina is now continuous over the dorsal neural tube on the contralateral control side, we consistently observe disruption of laminin dorsolaterally on the cingulin-depleted side of the embryo. Importantly, this loss of laminin is correlated with the noted increase in the number of migratory neural crest cells. In the chick trunk and head, the basal lamina is

discontinuous and is not fully established over the dorsal neural tube until cessation of neural crest cell emigration (Martins-Green and Erickson, 1987; our data). Indeed, the former study finds that the basal lamina does not play a role in temporally regulating the onset of trunk neural crest cell emigration, as basal lamina was found deposited on premigratory neural crest cells and therefore does not impede emigration. Furthermore, additional work in chick has shown that neural crest cells do not penetrate basal laminae (Erickson, 1987). Early microscopy studies in the chick head, however, indicate the presence of basal lamina along the dorsalateral regions of premigratory neural crest cells, particularly at the time of cranial neural fold fusion, and document the loss of this basal lamina prior to emigration (Tosney, 1982). Penetration of the basal lamina in the mouse head has also been proposed to occur during neural crest cell migration (Nichols, 1981; Nichols, 1987).

The further loss of basal lamina and subsequent emigration of neural crest cells from more dorsolateral positions in the chick midbrain upon cingulin knockdown defines a possible cellular mechanism for the observed increase in the number of migratory neural crest cells. We hypothesize that cingulin may act, directly or indirectly, to negatively regulate the breakdown of the dorsalateral neural tube basal lamina. This role could be accomplished through an association with the cytoskeleton, with proteins that interact with the basal lamina, and/or through the regulation of proteases, such as plasminogen activator (Valinsky and Le Douarin, 1985; Kalcheim and Le Douarin, 1999), which have been proposed to function in premigratory and/or early emigrating neural crest cells to degrade components of the basal lamina and promote emigration. As such, cingulin depletion leads to further dorsolateral loss of basal lamina, thereby physically freeing up additional regions in the dorsolateral neural tube through which premigratory neural crest cells can emerge and migrate. In keeping with this, we observe no change in the distribution of the premigratory neural crest cell Cadherin, Cad6B, or in the tight junction markers claudin-1 and ZO-1, indicating that alterations in cingulin are not directly affecting other junctional components. These latter results also imply that cingulin may modulate neural crest cell migration through a function that is separate from its role as a tight junction component. As not all neural tube cells receive the MO (due to intrinsic variations in the electroporation/transfection technique) and thus preclude *cingulin* mRNA translation, the observed effect on neural crest cell migration is notable and reflects the efficiency with which MO-mediated knockdown can be achieved in the developing chick midbrain. This work is the first to reveal a functional role for cingulin *in vivo* with respect to regulating chick midbrain neural crest cell migration.

Forced expression of cingulin expands the migratory neural crest cell population *in vivo*, which is associated with changes in the basal lamina and premigratory neural crest cell domain

Cingulin overexpression in the developing chick midbrain neuroepithelium results in a range of phenotypes, including effects on neural crest cell migration, cellular delamination, and the localization of cingulin protein. One specific observation is the presence of cells in the neural tube lumen that are both positive and negative for neural crest molecular markers. We hypothesize that some of these negative cells were initially positive, and that we have analyzed these embryos at a stage when cells have already down-regulated neural crest molecular markers and are undergoing apoptosis due to their inappropriate location in the neural tube lumen. In support of this hypothesis, we see *Sox10*-positive neural crest cells in the neural tube lumen after 20 hours of incubation following overexpression of cingulin, and, in other experiments, we observe cells in the lumen undergoing apoptosis. Alternatively, those cells in the lumen may be neural tube cells that have been forced into the lumen due to changes in neural tube architecture and/or cell death.

Comparable to our MO results, forced expression of cingulin also leads to an increase in the size of the migratory neural crest cell domain, but this occurs through a partially different mechanism than that observed upon cingulin knockdown. Although both cingulin depletion and overexpression correlate with loss of basal lamina, we also find that cingulin overexpression results in a statistically significant expansion of the premigratory neural crest cell domain, as assessed by the presence of increased numbers of *Snail2*- and *FoxD3*-positive cells in the dorsal neural folds. This expansion may result from transcriptional regulation of *Snail2* and *FoxD3* by cingulin due to its nuclear distribution upon overeexpression. Nuclear localization of cingulin has been reported previously for endogenous cingulin (Citi and Cordenonsi, 1999; Nakamura et al., 2000) and upon forced expression of the cingulin N-terminal head domain (D'Atri et al., 2002) in cultured cells. A potential role for a tight junction component in transcriptional regulation is not without precedence. The tight junction plaque protein symplekin has been shown to localize to the nucleus in non-epithelial cells and to both tight junctions and the nucleus in epithelial cells (Keon et al., 1996), where it plays a role in RNA polyadenylation and transcriptional regulation (Takagaki and Manley, 2000; Barnard et al., 2004; Kavanagh et al., 2006). It has been hypothesized that membrane-associated tight junction components such as symplekin and cingulin might exist in equilibrium with their respective cytoplasmic pools, with subsequent nuclear accumulation of these proteins reflecting a shift in the equilibrium to the cytoplasmic pool and, consequently, the movement of proteins to the nucleus (Citi and Cordenonsi, 1998). As such, it is possible that the mis-localization of cingulin to the nucleus upon overexpression leads to the formation of novel transcription factor complex(es) that positively regulate the expression of the premigratory neural crest cell markers *Snail2* and *FoxD3.* Further research is necessary, however, to address a potential function for cingulin as a transcriptional regulator during neural crest cell development in the chick midbrain.

In addition, our experimental results indicate that cingulin overexpression does not alter the levels or distribution of Cad6B, claudin-1, or ZO-1, again providing evidence that the mechanism by which cingulin controls neural crest cell migration is independent of cingulin function within the tight junctions. Cingulin overexpression is associated with loss of laminin, however, both dorsally (even after the basal lamina has been completely established on the contralateral control side of the embryo) and in ventrolateral regions of the neuroepithelium. This additional loss of laminin correlates with the emigration of neural crest cells from more dorsolateral regions of the neural tube as well as a decrease in RhoA protein levels ventrolaterally (see below). Taken together, all of these results provide a potential mechanistic explanation for the noted changes in neural crest cell migration.

The observation that both knock-down and overexpression of cingulin give a similar phenotype with respect to the correlative loss of laminin and increased numbers of migratory neural crest cells can be explained in at least two ways. First, it is not uncommon to observe comparable results upon overexpression and knock-down of the same molecule, as analogous phenotypes could very well reflect the requirement for the correct stoichiometry of complexes containing cingulin during neural crest cell development. It was recently shown that both overexpression and loss of Grhl2 give rise to neural tube defects in the mouse (Brouns et al., 2011), and this phenomenon has been generally observed for several molecules involved in regulating protein trafficking (Hrs (Bache et al., 2003; Morino et al., 2004); Rab13 (Nokes et al., 2008); Rab15 effector protein (Strick and Elferink, 2005); and Rab22a (Magadan et al., 2006)). Thus, we hypothesize that cingulin levels must be tightly controlled to prevent aberrant and premature emigration and migration of neural crest cells in the chick midbrain. Second, if cingulin is functioning to negatively regulate proteases that impinge upon the basal lamina in premigratory and/or early emigrating neural crest cells, then the aberrant localization of cingulin after overexpression (e.g. in the nucleus) may preclude cingulin from carrying out its normal functions in the cell, leading indirectly to

basal lamina depletion. This loss of basal lamina could also be compounded by the presence of more premigratory neural crest cells expressing proteases that may, in turn, degrade the basal lamina.

Basal lamina loss in the ventrolateral, but not dorsal, neuroepithelium is correlated with cingulin modulation of RhoA

During neural crest cell EMT, premigratory neural crest cells must dismantle cellular junctions in order to facilitate their egress from the dorsal neural tube. This process results in changes in cell morphology because cells lose epithelial characteristics and adopt a mesenchymal phenotype as they emigrate. In other developmental EMTs such as gastrulation, breakdown of the basal lamina is critical as cells detach and initiate movement (Nakaya et al., 2008). During chick gastrulation, this disruption of basal lamina involves the down-regulation of RhoA (Nakaya et al., 2008). Studies in cultured cells have shown that cingulin binds the Rho Guanine Exchange Factor GEF-H1 (Citi et al., 2009) and inhibits GEF-H1 activity, thus leading to the inactivation of RhoA and serving to couple the formation of tight junctions to a reduction in RhoA signaling (Aijaz et al., 2005). As such, we sought to determine whether the delamination we observe dorsally and ventrolaterally in the neuroepithelium could be correlated with changes in RhoA upon perturbation of cingulin.

RhoA is expressed apically as the neural plate invaginates to form the neural tube and co-localizes with actomyosin; however, RhoA is reduced apically in the posterior neural tube after neural tube closure, particularly in the dorsal region from which neural crest cells will delaminate (Kinoshita et al., 2008). As neural crest cells undergo EMT in the chick midbrain, we continually find diminished RhoA protein dorsally, with maintained apical distribution throughout the more ventrolateral neuroepithelium, in keeping with previous work (Kinoshita et al., 2008). Furthermore, we observe no change in RhoA levels dorsally upon perturbation of cingulin, suggesting that cingulin does not modulate RhoA in premigratory neural crest cells. Depletion and overexpression of cingulin outside of the dorsal region of the neural tube, however, lead to up- and down-regulation of RhoA, respectively, consistent with prior results in MDCK cells (Aijaz et al., 2005). Interestingly, the loss of RhoA observed upon cingulin overexpression is correlated with basal lamina breakdown in more ventrolateral regions of the neuroepithelium.

It is intriguing that loss of cingulin in the ventrolateral neuroepithelium upon *Cingulin* MO treatment does not lead to subsequent changes in the basal lamina (as what is seen dorsally). A potential molecular association between RhoA and the basal lamina, however, could explain these results. If down-regulation of RhoA in the neural tube were tied to the loss and/or breakdown of the basal lamina (similar to chick gastrulation), then elevation of RhoA levels, as observed in the ventolateral neuroepithelium upon cingulin knock-down, would preclude basal lamina disruption in this region. This is, in fact, the phenotype we observe upon cingulin depletion in the ventrolateral neuroepithelium. As such, our current working model is that cingulin regulates RhoA solely in the ventrolateral neuroepithelium due to the presence of appropriate RhoA GEFs in this specific region. This regulation ensures that RhoA is present in the apical neural tube and thus precludes aberrant and ectopic delamination of ventrolateral neuroepithelial cells. Loss of this regulation is apparent upon perturbation of cingulin, with overexpression of cingulin leading to decreased RhoA, loss of basal lamina, and ectopic ventrolateral neuroepithelial cell delamination, while depletion of cingulin causes up-regulation of RhoA levels with no subsequent effect on delamination. In premigratory neural crest cells in the dorsal neural tube, however, cingulin does not modulate RhoA levels, possibly due to the absence and/or inactivity of RhoA GEFs in this region, but cingulin does function to regulate neural crest cell emigration and migration. Additional research is necessary to define the molecular interactions among cingulin, RhoA,

and the basal lamina within various regions of the neuroepithelium, but the potential differential localization of diverse GEFs that interact with cingulin to modulate RhoA function could provide further insight to this regulation (Aijaz et al., 2005; Terry et al., 2011).

This study demonstrates that junctional proteins like cingulin can perform multiple functions during vertebrate development and further illustrates their general importance in the embryo. Our work suggests that cingulin modulates cellular delamination through a mechanism that can be partially correlated with additional disruption of the basal lamina. Collectively, our findings have uncovered a novel role for a tight junction-associated protein in regulating neural crest cell migration in the chick midbrain.

EXPERIMENTAL PROCEDURES

Chicken embryo culture

Fertilized chicken eggs were obtained from Hy-Line North America, L.L.C. (Elizabethtown, PA) or B & E Farms (York, PA) and incubated at 38°C in humidified incubators (EggCartons.com, Manchaug, MA). Embryos were staged according to the number of pairs of somites.

Design and electroporation of cingulin antisense morpholino

A 3′ lissamine-labeled antisense *Cingulin* morpholino (MO), 5′-GCCGTGCGCTCCATGCCGGGTGC-3′, was designed to target the *cingulin* mRNA according to the manufacturer's criteria (GeneTools, L.L.C.). A 5 base pair mismatch lissamine-labeled antisense *Cingulin* control MO 5′-GCgGTcCGCTCgATGCCGcGTcC-3′ (mutated bases are in lower case; GeneTools, L.L.C.) was used that does not target *cingulin* mRNA. MOs were introduced into the developing chick embryo using a modified version of the electroporation technique (Itasaki et al., 1999). Briefly, MOs were injected at a final concentration of 500 μM (Taneyhill et al., 2007; Jhingory et al., 2010) into the neural tube lumen at the desired axial level and 2, 25 volt, 30 mSec pulses were applied across the embryo.

Overexpression of cingulin in vivo

The full-length *cingulin* cDNA was directionally cloned into the pCIG chick expression construct by PCR using a chick cDNA library (7–12ss) as the template in order to produce pCIG-Cingulin, and sequenced to confirm accuracy. The control (pCIG) or pCIG-Cingulin expression construct was introduced into the embryo at a concentration of 3 μg/μl, as described above for the MO electroporations.

Whole-mount in situ hybridization

Whole-mount *in situ* hybridization was performed as described previously in (Wilkinson, 1992; Coles et al., 2007; Taneyhill et al., 2007). Stained embryos were viewed in whole-mount at room temperature in 70% glycerol using a Zeiss SteREO Discovery.V8 compound fluorescent microscope. Images were captured using the Zeiss Axiovision Rel 4.6 software with the Zeiss Axiocam MRc5 camera. Transverse-sections were obtained by cryostat-sectioning gelatin-embedded embryos at 14 μm in a Leico Frigocut or Fisher Microm cryostat, and coverslips were mounted on processed sections using Fluoromount G (Fisher). Sections were viewed at room temperature using a Zeiss AxioObserver.Z1 inverted microscope, and images were acquired using the Zeiss Axiovision Rel 4.6 software with the Zeiss Axiocam HRC camera. All exported images were processed in Adobe Photoshop 9.0 (Adobe Systems).

Immunohistochemistry

Immunohistochemical detection of various proteins was performed in whole-mount or on transverse sections following 4% paraformaldehyde fixation of embryos and cryostat-sectioning, as in (Nakagawa and Takeichi, 1998; Coles et al., 2007; Taneyhill et al., 2007; Jhingory et al., 2010). The following primary antibodies and concentrations were used in the experiments: Cingulin (Invitrogen #36–4401; 1:350), RhoA (Lulu 51, a kind gift from Dr. Shigenobu Yonemura, RIKEN, or Santa Cruz #sc-418; both at 1:300; slides treated with 0.1M sodium citrate for 20 minutes at 96°C and washed three times with PBS + 0.1% TX-100 prior to blocking), Cad6B (Developmental Studies Hybridoma Bank (DSHB), clone CCD6B-1; 1:100), laminin (DSHB, clone 3H11; 1:100), claudin-1 (Invitrogen #37–4900, 1:200, using 1X PBS + 0.2% TX-100, supplemented with 1% BSA for blocking), ZO-1 (Zymed 40–2300; 1:300), phospho-histone H3 (Millipore Ser10; 1:500), GFP (Invitrogen A11122 or A11121; 1:500) and HNK-1 (1:100). Appropriate fluorescently-conjugated secondary antibodies (Alexa 488 or 594) from Invitrogen were used at a concentration of 1:200 to 1:1000. Imaging of sections and data processing were carried out as described above for *in situ* hybridizations using the Zeiss AxioObserver.Z1 inverted microscope and Adobe Photoshop 9.0 (Adobe Systems), respectively. Sections were stained with DAPI to mark cell nuclei and mounted using Fluoromount G (Fisher).

Cell counts

Cell counts of *Sox10*, *Snail-2*, or *FoxD3*-expressing cells in sections were performed as described previously (Coles et al., 2007; Jhingory et al., 2010). Briefly, embryos electroporated with control MO, *Cingulin* MO, pCIG or pCIG-Cingulin and hybridized with a *Sox10*, *Snail2*, or *FoxD3*-antisense riboprobe were imaged and subsequently cryostat-sectioned at 14 μm. Sections were stained with DAPI to enable the identification of individual nuclei and mounted for imaging using Fluoromount G (Fisher). 7–10 serial images from the midbrain were captured in a minimum of 3 embryos that had MO or GFP localized to the dorsal neural tube (and thus successfully transfected). All DAPI-positive nuclei surrounded by cytoplasmic *Sox10* in the migratory neural crest cell streams (or *Snail2* and *FoxD3* in premigratory neural crest cells in the dorsal neural tube) on both the electroporated and non-electroporated side were counted and recorded. Fold differences were then averaged over the number of sections in which cells were counted, and the standard error of the mean was calculated and compared for embryos electroporated with either control MO, *Cingulin* MO, pCIG or pCIG-Cingulin. Significance of results was established using the unpaired Student's *t* test.

Quantification of RhoA immunofluorescence

Quantification of RhoA intensity in the apical region of the neural tube was carried out using the "outline spline" function of the Zeiss Axiovision Rel 4.6 software. This function allows for the calculation of a densitometric mean (normalized to area) of the region of interest for a particular channel after subtraction of background. By outlining the apical region of the neural tube in at least 5 serial sections in a minimum of 7 embryos, densitometric means were calculated for RhoA on both the treated and contralateral control sides of each section. An overall mean was then obtained and fold change was calculated. The unpaired Student's *t* test was used to assess data significance.

Supplementary Material

Refer to Web version on PubMed Central for supplementary material.

Acknowledgments

Grant sponsor: NIH; Grant number: HD055034

Grant sponsor: NSF; Grant number: IOS-0948525

We thank Dr. Edward Coles for critically reading the manuscript. The Cad6B and laminin antibodies were obtained from the DSHB developed under the auspices of the NICHD and maintained by The University of Iowa, Department of Biology, Iowa City, IA 52242. The RhoA antibody Lulu 51 was a kind gift from Dr. Shigenobu Yonemura, RIKEN. This research was supported by grants from the NIH (R00 HD055034) and NSF (IOS-0948525) to L.A.T.

References

Aaku-Saraste E, Hellwig A, Huttner WB. Loss of occludin and functional tight junctions, but not ZO-1, during neural tube closure--remodeling of the neuroepithelium prior to neurogenesis. Dev Biol. 1996; 180:664–679. [PubMed: 8954735]

Acloque H, Adams MS, Fishwick K, Bronner-Fraser M, Nieto MA. Epithelial-mesenchymal transitions: the importance of changing cell state in development and disease. J Clin Invest. 2009; 119:1438–1449. [PubMed: 19487820]

Ahlstrom JD, Erickson CA. The neural crest epithelial-mesenchymal transition in 4D: a ‘tail’ of multiple non-obligatory cellular mechanisms. Development. 2009; 136:1801–1812. [PubMed: 19429784]

Aijaz S, D’Atri F, Citi S, Balda MS, Matter K. Binding of GEF-H1 to the tight junction-associated adaptor cingulin results in inhibition of Rho signaling and G1/S phase transition. Dev Cell. 2005; 8:777–786. [PubMed: 15866167]

Bache KG, Raiborg C, Mehlum A, Stenmark H. STAM and Hrs are subunits of a multivalent ubiquitin-binding complex on early endosomes. J Biol Chem. 2003; 278:12513–12521. [PubMed: 12551915]

Barnard DC, Ryan K, Manley JL, Richter JD. Symplekin and xGLD-2 are required for CPEB-mediated cytoplasmic polyadenylation. Cell. 2004; 119:641–651. [PubMed: 15550246]

Barrallo-Gimeno A, Nieto MA. The Snail genes as inducers of cell movement and survival: implications in development and cancer. Development. 2005; 132:3151–3161. [PubMed: 15983400]

Brouns MR, De Castro SC, Terwindt-Rouwenhorst EA, Massa V, Hekking JW, Hirst CS, Savery D, Munts C, Partridge D, Lamers W, Kohler E, van Straaten HW, Copp AJ, Greene ND. Over-expression of Grhl2 causes spina bifida in the Axial defects mutant mouse. Hum Mol Genet. 2011; 20:1536–1546. [PubMed: 21262862]

Cardellini P, Cirelli A, Citi S. Tight junction formation in early Xenopus laevis embryos: identification and ultrastructural characterization of junctional crests and junctional vesicles. Cell Tissue Res. 2007; 330:247–256. [PubMed: 17786481]

Cardellini P, Davanzo G, Citi S. Tight junctions in early amphibian development: detection of junctional cingulin from the 2-cell stage and its localization at the boundary of distinct membrane domains in dividing blastomeres in low calcium. Dev Dyn. 1996; 207:104–113. [PubMed: 8875080]

Citi S, Cordenonsi M. Tight junction proteins. Biochim Biophys Acta. 1998; 1448:1–11. [PubMed: 9824655]

Citi S, Paschoud S, Pulimeno P, Timolati F, De Robertis F, Jond L, Guillemot L. The tight junction protein cingulin regulates gene expression and RhoA signaling. Ann N Y Acad Sci. 2009; 1165:88–98. [PubMed: 19538293]

Citi S, Sabanay H, Jakes R, Geiger B, Kendrick-Jones J. Cingulin, a new peripheral component of tight junctions. Nature. 1988; 333:272–276. [PubMed: 3285223]

Citi S, Sabanay H, Kendrick-Jones J, Geiger B. Cingulin: characterization and localization. J Cell Sci. 1989; 93 (Pt 1):107–122. [PubMed: 2693465]

Coles EG, Taneyhill LA, Bronner-Fraser M. A critical role for Cadherin6B in regulating avian neural crest emigration. Dev Biol. 2007; 312:533–544. [PubMed: 17991460]

Cordenonsi M, D'Atri F, Hammar E, Parry DA, Kendrick-Jones J, Shore D, Citi S. Cingulin contains globular and coiled-coil domains and interacts with ZO-1, ZO-2, ZO-3, and myosin. J Cell Biol. 1999; 147:1569–1582. [PubMed: 10613913]

D'Atri F, Citi S. Cingulin interacts with F-actin in vitro. FEBS Lett. 2001; 507:21–24. [PubMed: 11682052]

D'Atri F, Nadalutti F, Citi S. Evidence for a functional interaction between cingulin and ZO-1 in cultured cells. J Biol Chem. 2002; 277:27757–27764. [PubMed: 12023291]

De Craene B, van Roy F, Berx G. Unraveling signalling cascades for the Snail family of transcription factors. Cellular Signaling. 2005; 17:535–547.

Erickson A. Behavior of neural crest cells on embryonic basal laminae. Dev Biol. 1987; 120:38–49. [PubMed: 3817299]

Fesenko I, Kurth T, Sheth B, Fleming TP, Citi S, Hausen P. Tight junction biogenesis in the early Xenopus embryo. Mech Dev. 2000; 96:51–65. [PubMed: 10940624]

Fleming TP, Hay M, Javed Q, Citi S. Localisation of tight junction protein cingulin is temporally and spatially regulated during early mouse development. Development. 1993; 117:1135–1144. [PubMed: 8325238]

Groysman M, Shoval I, Kalcheim C. A negative modulatory role for rho and rho-associated kinase signaling in delamination of neural crest cells. Neural Dev. 2008; 3:27. [PubMed: 18945340]

Guillemot L, Citi S. Cingulin regulates claudin-2 expression and cell proliferation through the small GTPase RhoA. Mol Biol Cell. 2006; 17:3569–3577. [PubMed: 16723500]

Hay ED. An overview of epithelio-mesenchymal transformation. Acta Anat (Basel). 1995; 154:8–20. [PubMed: 8714286]

Hemavathy K, Guru SC, Harris J, Chen JD, Ip YT. Human Slug is a repressor that localizes to sites of active transcription. Mol Cell Bio. 2000; 26:5087–5095. [PubMed: 10866665]

Hemavathy K, Hu X, Ashraf SI, Small SJ, Ip YT. The repressor function of snail is required for Drosophila gastrulation and is not replaceable by Escargot or Worniu. Dev Biol. 2004; 269:411–420. [PubMed: 15110709]

Ikenouchi J, Matsuda M, Furuse M, Tsukita S. Regulation of tight junctions during the epithelium-mesenchyme transition: direct repression of the gene expression of claudins/occludin by Snail. J Cell Sci. 2003; 116:1959–1967. [PubMed: 12668723]

Itasaki N, Bel-Vialar S, Krumlauf R. 'Shocking' developments in chick embryology: electroporation and in ovo gene expression. Nat Cell Biol. 1999; 1:E203–207. [PubMed: 10587659]

Javed Q, Fleming TP, Hay M, Citi S. Tight junction protein cingulin is expressed by maternal and embryonic genomes during early mouse development. Development. 1993; 117:1145–1151. [PubMed: 8325239]

Jhingory S, Wu CY, Taneyhill LA. Novel insight into the function and regulation of alphaN-catenin by Snail2 during chick neural crest cell migration. Dev Biol. 2010; 344:896–910. [PubMed: 20542025]

Kalcheim, C.; Le Douarin, N. The neural crest. New York: Cambridge University Press; 1999.

Kavanagh E, Buchert M, Tsapara A, Choquet A, Balda MS, Hollande F, Matter K. Functional interaction between the ZO-1-interacting transcription factor ZONAB/DbpA and the RNA processing factor symplekin. J Cell Sci. 2006; 119:5098–5105. [PubMed: 17158914]

Keon BH, Schafer S, Kuhn C, Grund C, Franke WW. Symplekin, a novel type of tight junction plaque protein. J Cell Biol. 1996; 134:1003–1018. [PubMed: 8769423]

Kinoshita N, Sasai N, Misaki K, Yonemura S. Apical accumulation of Rho in the neural plate is important for neural plate cell shape change and neural tube formation. Mol Biol Cell. 2008; 19:2289–2299. [PubMed: 18337466]

Leptin M, Casal J, Grunewald B, Reuter R. Mechanisms of early Drosophila mesoderm formation. Dev Suppl. 1992:23–31. [PubMed: 1299365]

Liu J-P, Jessell T. A role for rhoB in the delamination of neural crest cells from the dorsal neural tube. Development. 1998; 125:5055–5067. [PubMed: 9811589]

Magadan JG, Barbieri MA, Mesa R, Stahl PD, Mayorga LS. Rab22a regulates the sorting of transferrin to recycling endosomes. Mol Cell Biol. 2006; 26:2595–2614. [PubMed: 16537905]

Martinez-Estrada OM, Culleres A, Soriano FX, Peinado H, Bolos V, Martinez FO, Reina M, Cano A, Fabre M, Vilaro S. The transcription factors Slug and Snail act as repressors of Claudin-1 expression in epithelial cells. Biochem J. 2006; 394:449–457. [PubMed: 16232121]

Martins-Green M, Erickson CA. Basal lamina is not a barrier to neural crest cell emigration: documentation by TEM and by immunofluorescent and immunogold labelling. Development. 1987; 101:517–533. [PubMed: 3332260]

Morino C, Kato M, Yamamoto A, Mizuno E, Hayakawa A, Komada M, Kitamura N. A role for Hrs in endosomal sorting of ligand-stimulated and unstimulated epidermal growth factor receptor. Exp Cell Res. 2004; 297:380–391. [PubMed: 15212941]

Nakagawa S, Takeichi M. Neural crest emigration from the neural tube depends on regulated cadherin expression. Development. 1998; 125:2963–2971. [PubMed: 9655818]

Nakamura T, Blechman J, Tada S, Rozovskaia T, Itoyama T, Bullrich F, Mazo A, Croce CM, Geiger B, Canaani E. huASH1 protein, a putative transcription factor encoded by a human homologue of the Drosophila ash1 gene, localizes to both nuclei and cell-cell tight junctions. Proc Natl Acad Sci U S A. 2000; 97:7284–7289. [PubMed: 10860993]

Nakaya Y, Sukowati EW, Wu Y, Sheng G. RhoA and microtubule dynamics control cell-basement membrane interaction in EMT during gastrulation. Nat Cell Biol. 2008; 10:765–775. [PubMed: 18552836]

Nichols DH. Neural crest formation in the head of the mouse embryo as observed using a new histological technique. J Embryol Exp Morphol. 1981; 64:105–120. [PubMed: 7031165]

Nichols DH. Ultrastructure of neural crest formation in the midbrain/rostral hindbrain and preotic hindbrain regions of the mouse embryo. Am J Anat. 1987; 179:143–154. [PubMed: 3618526]

Niessen CM. Tight junctions/adherens junctions: basic structure and function. J Invest Dermatol. 2007; 127:2525–2532. [PubMed: 17934504]

Nieto MA. The Snail superfamily of zinc-finger transcription factors. Nature Reviews: Molecular Cell Biology. 2002; 3:155–166.

Nokes RL, Fields IC, Collins RN, Folsch H. Rab13 regulates membrane trafficking between TGN and recycling endosomes in polarized epithelial cells. J Cell Biol. 2008; 182:845–853. [PubMed: 18779367]

Ohkubo T, Ozawa M. The transcription factor Snail downregulates the tight junction components independently of E-cadherin downregulation. J Cell Sci. 2004; 117:1675–1685. [PubMed: 15075229]

Perez-Mancera PA, Gonzalez-Herrero I, Perez-Caro M, Gutierrez-Cianca N, Flores T, Gutierrez-Adan A, Pintado B, Snachez-Martin M, Sanchez-Garcia I. SLUG in cancer development. Oncogene. 2005; 24:3073–3082. [PubMed: 15735690]

Sauka-Spengler T, Bronner-Fraser M. A gene regulatory network orchestrates neural crest formation. Nat Rev Mol Cell Biol. 2008; 9:557–568. [PubMed: 18523435]

Strick DJ, Elferink LA. Rab15 effector protein: a novel protein for receptor recycling from the endocytic recycling compartment. Mol Biol Cell. 2005; 16:5699–5709. [PubMed: 16195351]

Takagaki Y, Manley JL. Complex protein interactions within the human polyadenylation machinery identify a novel component. Mol Cell Biol. 2000; 20:1515–1525. [PubMed: 10669729]

Taneyhill LA, Coles EG, Bronner-Fraser M. Snail2 directly represses cadherin6B during epithelial-to-mesenchymal transitions of the neural crest. Development. 2007; 134:1481–1490. [PubMed: 17344227]

Terry SJ, Zihni C, Elbediwy A, Vitello E, Leefa Chong San IV, Balda MS, Matter K. Spatially restricted activation of RhoA signalling at epithelial junctions by p114RhoGEF drives junction formation and morphogenesis. Nat Cell Biol. 2011; 13:159–166. [PubMed: 21258369]

Thiery JP. Epithelial-mesenchymal transitions in tumour progression. Nat Rev Cancer. 2002; 2:442–454. [PubMed: 12189386]

Tosney KW. The segregation and early migration of cranial neural crest cells in the avian embryo. Dev Biol. 1982; 89:13–24. [PubMed: 7054004]

Valinsky JE, Le Douarin NM. Production of plasminogen activator by migrating cephalic neural crest cells. EMBO J. 1985; 4:1403–1406. [PubMed: 4040851]

Wilkinson, DG. Whole mount in situ hybridization of vertebrate embryos. In: Wilkinson, DG., editor. In Situ Hybridization. Oxford: Oxford University Press; 1992. p. 75-83.

Wu SY, McClay DR. The Snail repressor is required for PMC ingression in the sea urchin embryo. Development. 2007; 134:1061–1070. [PubMed: 17287249]

Yang J, Weinberg RA. Epithelial-mesenchymal transition: at the crossroads of development and tumor metastasis. Dev Cell. 2008; 14:818–829. [PubMed: 18539112]

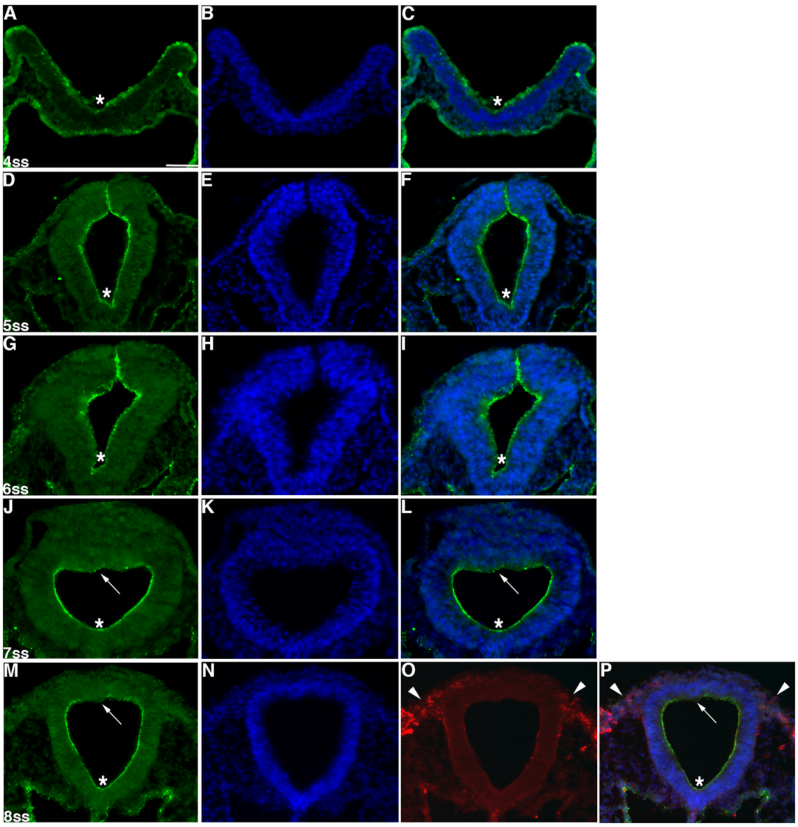

Figure 1. Cingulin protein distribution in the developing chick embryo midbrain

(A, D, G, J, M) Transverse sections taken through the chick embryo midbrain following whole-mount immunohistochemistry for cingulin, with representative sections shown for specific developmental stages (A–C, 4ss; D–F, 5ss; G–I, 6ss; J–L, 7ss; M–P, 8ss). (B, E, H, K, N) DAPI staining (blue) of (A, D, G, J, M) to mark cell nuclei. (C, F, I, L, P) Merge images. Asterisks indicate apical localization of cingulin, with diminished apical distribution of cingulin dorsally noted by arrows at the 7ss (J, L) and 8ss (M, P). HNK-1 immunostaining (red) of migratory neural crest cells is shown in (O, P; arrowheads) at 8ss. Scale bar is 50 μm and is applicable to all section images.

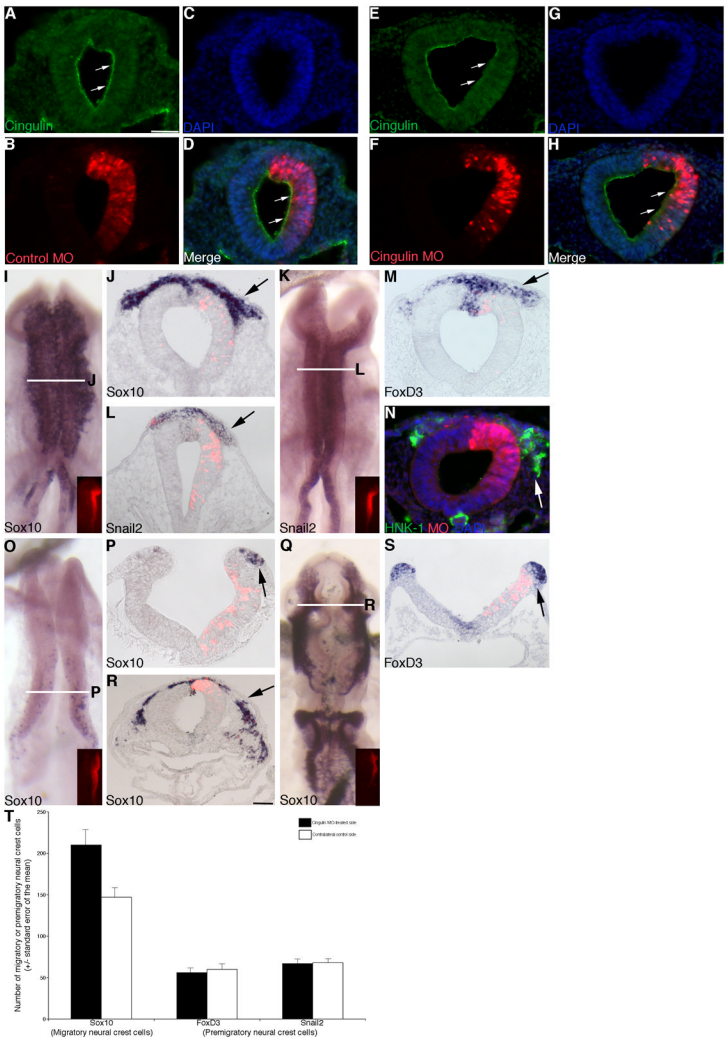

Figure 2. Morpholino-mediated depletion of cingulin from the developing neural crest cell population of the chick midbrain expands the size of the migratory neural crest cell domain

(A–C, E–G) Individual channel and (D, H) merge images of a representative transverse section taken through an embryo electroporated with the Control or *Cingulin* MO (red), respectively, after 8 hours of MO incubation and processing by immunohistochemistry for cingulin protein (A, D, F, H, green). Apical localization of cingulin in the neural tube is indicated by the arrows (A, D, E, H). (I, K) Whole-mount *in situ* hybridization followed by indicated transverse sections for *Sox10* (J) and *Snail2* (L), respectively, after 8 hour incubation following treatment with *Cingulin* MO. (M, N) Representative transverse sections taken from embryos treated with *Cingulin* MO for 8 hours followed by *FoxD3* whole-mount *in situ* hybridization (M) or immunohistochemistry for HNK-1 (N, green), respectively. (O, Q) Whole-mount *in situ* hybridization followed by indicated transverse section (P, R) for *Sox10* after 3 and 20 hour incubation following treatment with *Cingulin* MO, respectively. (S) Representative transverse section taken from an embryo treated with *Cingulin* MO for 3 hours followed by *FoxD3* whole-mount *in situ* hybridization. (T) Graphical representation of the increase in migratory neural crest cells (*Sox10*) observed upon *Cingulin* MO treatment, with no change noted in the premigratory neural crest cell population (*FoxD3*, *Snail2*). Arrows in (I–S) indicate the migratory or premigratory neural crest cell domain. In all experiments, the right side of the embryo is electroporated, as

indicated by the lissamine (red) fluorescence of the MO in the transverse sections (B, D, F, H, J, L, M, N, P, R, S) and/or in the inset images of each whole-mount (I, K, O, Q). Scale bar in (A) is 50 μm and applicable to all whole-mount and section images except for that shown in (R) where the scale bar is also 50 μm. DAPI, blue.

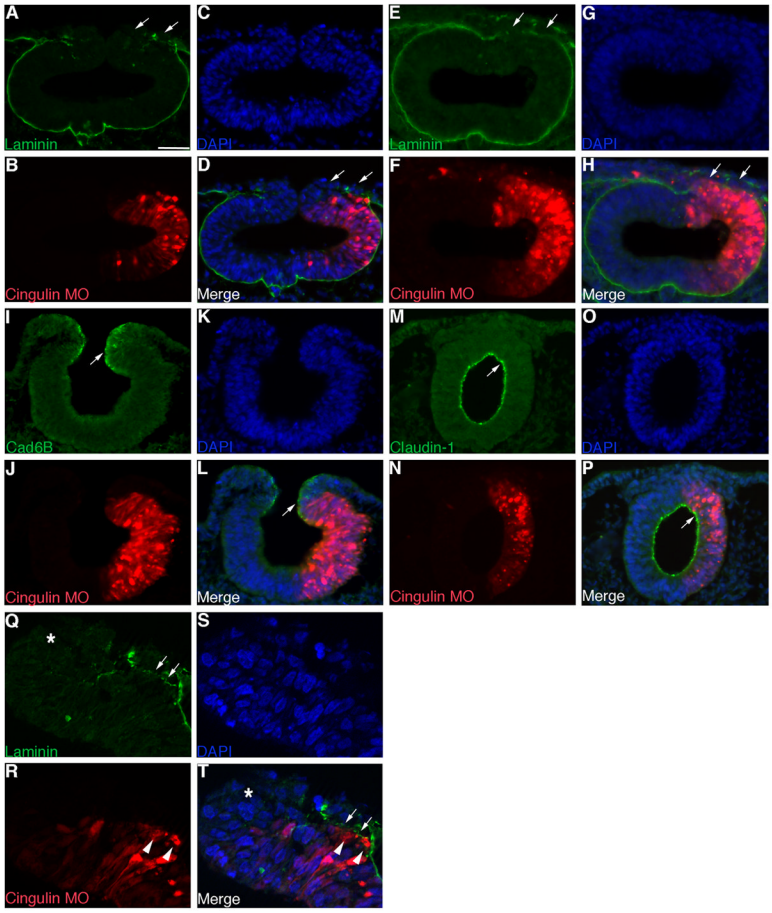

Figure 3. Morpholino-mediated depletion of cingulin from the developing neural crest cell population of the chick midbrain is correlated with loss of laminin and maintained adherens and tight junctions

(A–C, E–G, I–K, M–O) Individual channel and (D, H, L, P) merge images of a representative transverse section taken through an embryo electroporated with *Cingulin* MO (red) after 3 (A–D, I–L) and 8 (E–H, M–P) hours of MO incubation and processing by immunohistochemistry for laminin (A, D, E, H), Cad6B (I, L), and claudin-1 (M, P) (all green), respectively. Arrows point to a loss of laminin (A, D, E, H) or denote Cad6B or claudin-1 on the transfected side of the neural tube. (Q–S) Individual channel and (T) merge high resolution images of a representative transverse section taken through an embryo electroporated with *Cingulin* MO (red) after 3 hours of MO incubation and processing by immunohistochemistry for laminin. Arrows, arrowheads, and asterisks point to dorsolateral loss of laminin, emigrating neural crest cells, and the location of the dorsal neural tube, respectively. In all experiments, the right side of the embryo is electroporated, as indicated by the lissamine (red) fluorescence of the MO in the transverse sections. Scale bar in (A) is 50 μm and applicable to all section images. DAPI, blue.

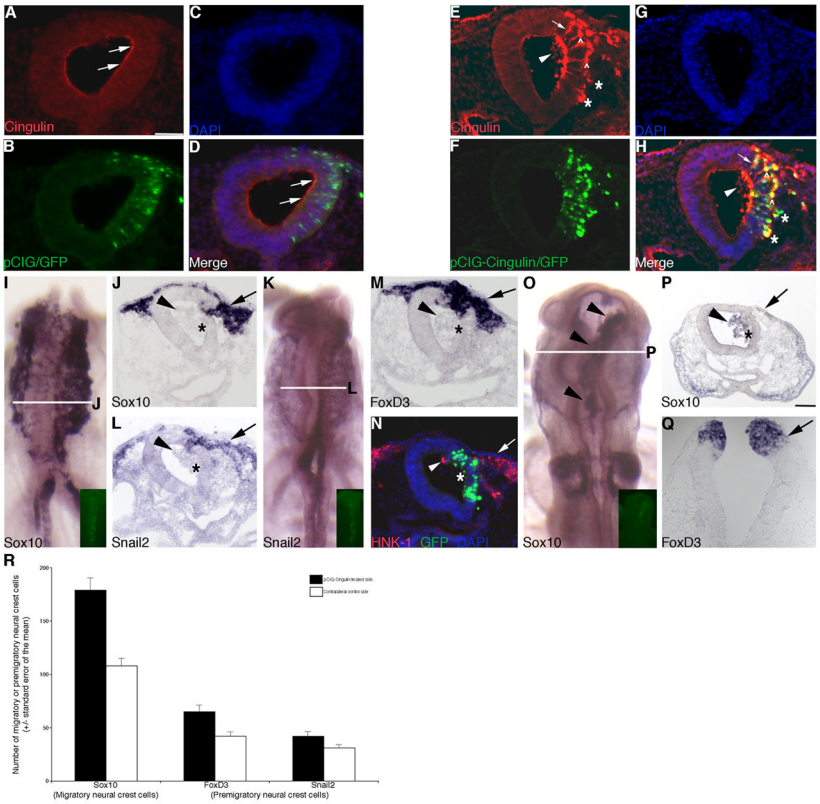

Figure 4. Overexpression of cingulin in the developing neural crest cell population of the chick midbrain increases the size of the migratory neural crest cell domain

(A–C, E–G) Individual channel and (D, H) merge images of a representative transverse section taken through an embryo electroporated with the pCIG control or pCIG-Cingulin construct (green), respectively, after 8 hours of incubation and subsequent processing by immunohistochemistry for cingulin protein (red). Arrows, asterisks, carets and arrowheads indicate apical or lateral cingulin (A, D, E, H), multiple cingulin-positive, ectopically delaminating neuroepithelial cells (E, H), nuclear cingulin (E, H), and cells in the neural tube lumen (E, H). (I, K) Whole-mount *in situ* hybridization followed by indicated transverse sections for *Sox10* (J) and *Snail2* (L), respectively, after 8 hour incubation following treatment with pCIG-Cingulin. (M, N) Representative transverse sections taken from embryos treated with pCIG-Cingulin for 8 hours followed by *FoxD3* whole-mount *in situ* hybridization (M) or immunohistochemistry for HNK-1 (N, red), respectively. (O) Whole-mount *in situ* hybridization followed by indicated transverse section (P) for *Sox10* after 20 hour incubation following treatment with pCIG-Cingulin. Arrows, asterisks, and arrowheads in (I–P) denote the migratory neural crest cell domain, a disruption in neural tube architecture on the electroporated side of the embryo, and cells in the neural tube lumen, respectively. (Q) Representative transverse section taken from an embryo treated with pCIG-Cingulin for 6 hours followed by *FoxD3* whole-mount *in situ* hybridization. Arrow indicates the premigratory neural crest cell domain. (R) Graphical representation of the increase in the migratory (*Sox10*) and premigratory (*FoxD3*, *Snail2*) neural crest cell populations observed upon cingulin overexpression. In all experiments, the right side of the embryo is electroporated, as indicated by the GFP (green) fluorescence in (B, F, N) and in the inset images in (I, K, O). Scale bar in (A) is 50 μm and applicable to all whole-mount and section images except for (P) (scale bar for P is also 50 μm). DAPI, blue.

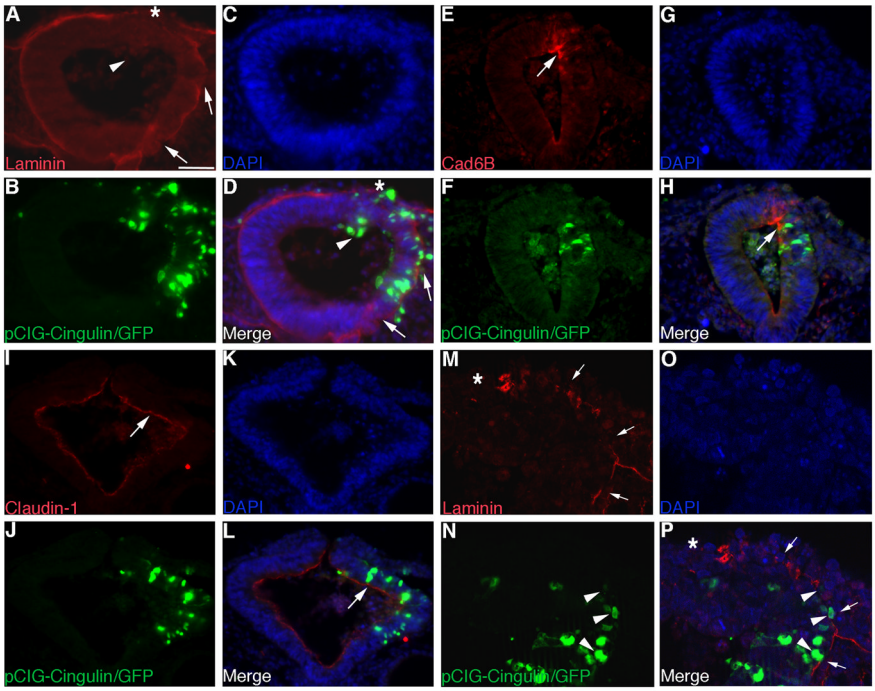

Figure 5. Overexpression of cingulin in the developing neural crest cell population of the chick midbrain is associated with loss of laminin in both dorsal and ventrolateral neuroepithelial cells and maintained adherens and tight junctions

(A–C, E–G, I–K) Individual channel and (D, H, L) merge images of a representative transverse section taken through an embryo electroporated with pCIG-Cingulin (green) after 8 (A–D) or 6 (E–L) hours of incubation and processing by immunohistochemistry for laminin (A, D), Cad6B (E, H) and claudin-1 (I, L) (all red), respectively. In (A, D), loss of laminin in the dorsal neural tube and ventrolateral neuroepithelium is indicated by asterisks and arrows, respectively, while arrowheads show cells in the neural tube lumen. Arrows in (E, H, I, L) denote Cad6B or claudin-1, respectively, on the transfected side of the neural tube. (M–O) Individual channel and (P) merge high resolution images of a representative transverse section taken through an embryo electroporated with pCIG-Cingulin (green) after 8 hours of incubation and processing by immunohistochemistry for laminin. Arrows, arrowheads, and asterisks point to dorsolateral loss of laminin, emigrating neural crest cells, and the location of the dorsal neural tube, respectively. In all experiments, the right side of the embryo is electroporated, as indicated by the GFP (green) fluorescence in the transverse sections. Scale bar in (A) is 50 μm and applicable to all section images. DAPI, blue.

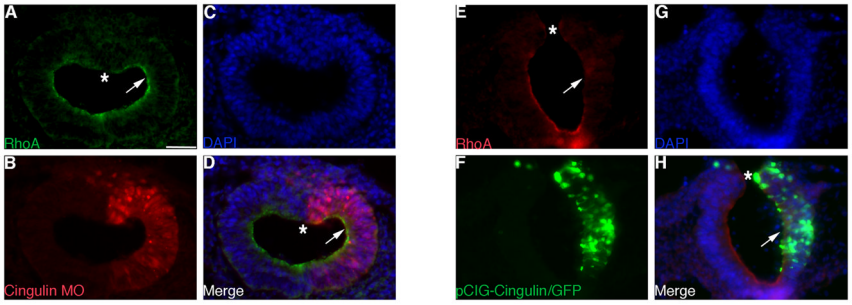

Figure 6. Perturbation of cingulin in the developing neural crest cell population of the chick midbrain alters RhoA protein distribution in ventrolateral neuroepithelial cells

(A–C, E–G) Individual channel and (D, H) merge images of representative transverse sections taken through an embryo electroporated with either *Cingulin* MO (A–D) or pCIG-Cingulin (E–H), respectively, after 8 hours of incubation and processing by immunohistochemistry for RhoA (A, D, green; E, H, red). Arrows and asterisks denote RhoA protein in the ventrolateral neuroepithelium and in the dorsal neural tube, respectively, on the electroporated side of the embryo. Scale bar for all images is indicated in (A) and is 50 μm. DAPI, blue.